

## Coaxial-Structured Solar Cells with Silicon Nanostructures

Hung-Hsien Li<sup>a</sup>, Kuan-Heng Chen<sup>b</sup>, Si-Ming Chiou<sup>c</sup>, Han-Wen Liu<sup>c</sup>, Chuan-Ping Juan<sup>b</sup>  
and Huang-Chung Cheng<sup>a</sup>

<sup>a</sup> Department of Electronics Engineering and Institute of Electronics, National Chiao Tung University, Hsinchu, 30010, Taiwan, R.O.C.

<sup>b</sup> Department of Electronics Engineering, St. John's University, Taipei 25135, Taiwan, R.O.C.

<sup>c</sup> Department of Electrical Engineering, National Chung Hsing University, Taichung 40227, Taiwan R.O.C.

Coaxial-structured solar cells with different lengths silicon nanowires (SiNWs) fabricated by e-beam lithography and transformer coupled plasma reactive ion etching (TCP-RIE) were demonstrated in this paper. With the intrinsic amorphous silicon thickness of 15 nm and n-layer thickness of 25 nm, the short-current density and the conversion efficiency of the flat film solar cell were 17.58 mA/cm<sup>2</sup> and 3.16 %, respectively. Furthermore, the short-current density increased from 20.75 to 27.90 mA/cm<sup>2</sup> and the conversion efficiency increased from 3.59 to 4.69 % when the silicon nanowires length was increased from 0.5 to 1 μm. The proposed coaxial-structured solar cells with SiNWs exhibited nearly 48.42 % efficiency enhancement over the flat film solar cell.

### Introduction

Many investigations had been focused on nanostructures and nanostructured materials for optoelectronic applications (1,2). Solar cells with nanostructures including nanoparticles, nanorods and nanowires have attracted much attention because of their potential for improving charge collection efficiency and serving as integrated power sources with device miniaturization (3,4).

Recently, vertical nanowire arrays have also been exploited in solar cells (5,6). Nanowire arrays structure more effectively absorbed sunlight, decreased the optical reflectance and increased the light trapping probability because of their larger aspect ratios. For this reason SiNWs arrays in particular have been intensely investigated into silicon based solar cells (7) in order to improve charge collection efficiency. There are many techniques available for the formation of SiNWs arrays, such as e-beam lithography (8), electroless metal deposition (9), pattern vapour-liquid-solid process (10), nanosphere lithography (11) and Langmuir–Blodgett assembly (12).

In this paper, e-beam lithography and TCP-RIE were proposed to fabricate the well-aligned silicon nanowires array. The coaxial-structured solar cells with SiNWs were sequentially capped with the intrinsic and n-layer amorphous silicon. The photovoltaic (PV) properties of the coaxial-structured solar cells with SiNWs and the flat film solar cell have been systematic discussed.

## Experimental

The SiNWs arrays were fabricated by e-beam lithography and TCP-RIE. First, a 100-nm-thick tetraethylorthosilicate (TEOS) oxide was deposited on the p-type (100) silicon substrate using a tube furnace. Second, a 400-nm-thick photoresist (PR) was spinning on the TEOS oxide. Next, a 100-nm-diameter PR array, which served as an etching mask, was patterned by e-beam lithography. Then, the TEOS oxide was etching using an oxide etcher and the residual PR was stripping by an ashing etcher. The TEOS oxide arrays were served as a mask for the SiNWs etching. Finally, the SiNWs were fabricated using TCP-RIE. The main etching conditions were using  $\text{Cl}_2$  (35 sccm) and  $\text{HBr}$  (125 sccm) as etching gases, transformer coupled plasma power of 310 W, bias power of 120 W and chamber pressure of 12 mTorr. The etching time was varied from 125 s to 250 s. The SiNWs length was controlled as 0.5 to 1  $\mu\text{m}$ .

After the SiNWs arrays were formed, they were sequentially capped with the i- and n-layer amorphous silicon by plasma-enhanced chemical vapor deposition (PECVD). The PECVD growth conditions were using  $\text{SiH}_4$  (10 sccm) source gas at a growth temperature of 350  $^\circ\text{C}$ ,  $\text{H}_2$  dilution ratio  $R$  ( $\text{H}_2/\text{SiH}_4$ )=10, deposition pressure of 700 mTorr, RF frequency of 40.68 MHz and  $\text{PH}_3$  (20 sccm) was utilized for n- doping. The thicknesses of the intrinsic and n-layer amorphous silicon were controlled as 15 nm and 25 nm, respectively. A 150-nm-thick ITO layer, which served as a transparent conduction layer, was deposited by magnetron sputtering at room temperature. Finally, a 600-nm-thick Al grid and a 50-nm-thick Pt, which served as the top and bottom electrodes, were deposited using e-gun evaporator and magnetron sputtering, accordingly. The Schematic diagram for process flow of the coaxial-structured solar cells with silicon nanowires is shown in Figure 1.

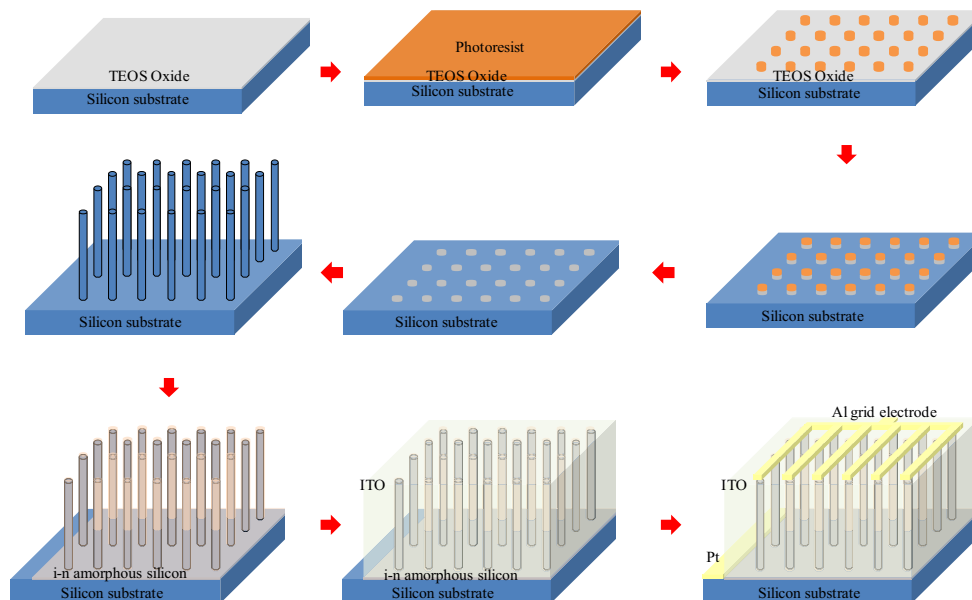
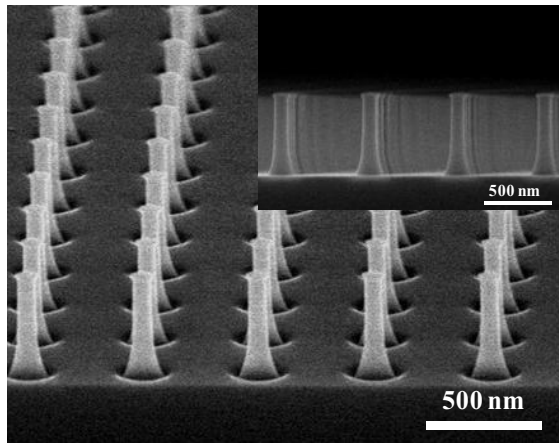


Figure 1. Schematic diagram for process flow of the coaxial-structured solar cells with silicon nanowires.

## Result and discussion

Figure 2 (a) shows the 45° tilted and cross-sectional (inset) field-emission scanning electron microscopy (FE-SEM) images of the as-fabricated SiNWs arrays using e-beam lithography and TCP-RIE. The dense well-aligned SiNWs were observed over the entire substrate. The average diameter and spacing of the SiNWs were around 100 nm and 500 nm, correspondingly. The wire length and structure of the SiNWs could be effectively controlled by adjusting etching conditions such as etching time, coupled plasma power and etching gases. The etching time is controlled as 125 s. The average wire length of the SiNWs is around 0.5  $\mu\text{m}$ . The 45° tilted and cross-sectional (inset) FE-SEM images of the SiNWs which were capped with i- and n-layer amorphous silicon are shown in Figure 2 (b). The SiNWs became larger and circular after i- and n-layer amorphous silicon deposited. It is conjectured that the individual SiNWs were conformally covered with the amorphous silicon. Approximately i-layer amorphous silicon thickness of 15 nm and n-layer one of 25 nm were deposited on the fabricated SiNWs arrays.

(a)



(b)

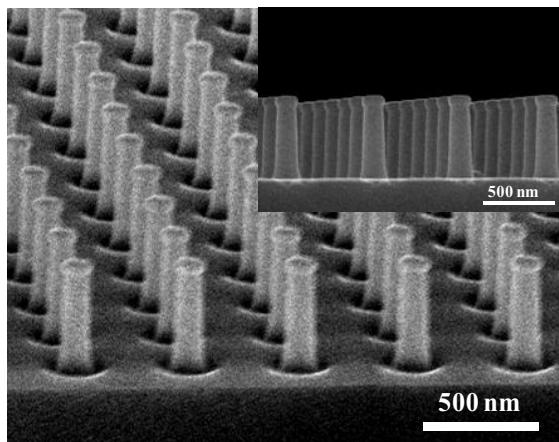


Figure 2. (a) 45° tilted and cross-sectional (inset) FE-SEM images of the as-fabricated SiNWs. (b) 45° tilted and cross-sectional (inset) FE-SEM images of the SiNWs capped with i- and n-layer amorphous silicon.

Transmission electron microscope (TEM) is employed to characterize the lattice structure and the crystallization of the fabricated SiNWs. Figure 3 (a) exhibits the low-magnification TEM image of a silicon nanowire and recognizes as along [100]. It illustrates that the diameter of the SiNWs were around 100 nm, which was consistent with the result from SEM observation. The high resolution transmission electron microscope (HRTEM) image of a silicon nanowire prepared from a (100) orientation silicon substrate is shown in figure 3 (b). Selective area electron diffraction (SAED) pattern in figure 3 (c) demonstrates the single-crystalline structure of the SiNWs. Figure 3 (d) reveals the EDS spectrum of the SiNWs. It has been found that the synthesized SiNWs contain only Si and O peaks. The small amount of Cu signals may come from the TEM copper grid.

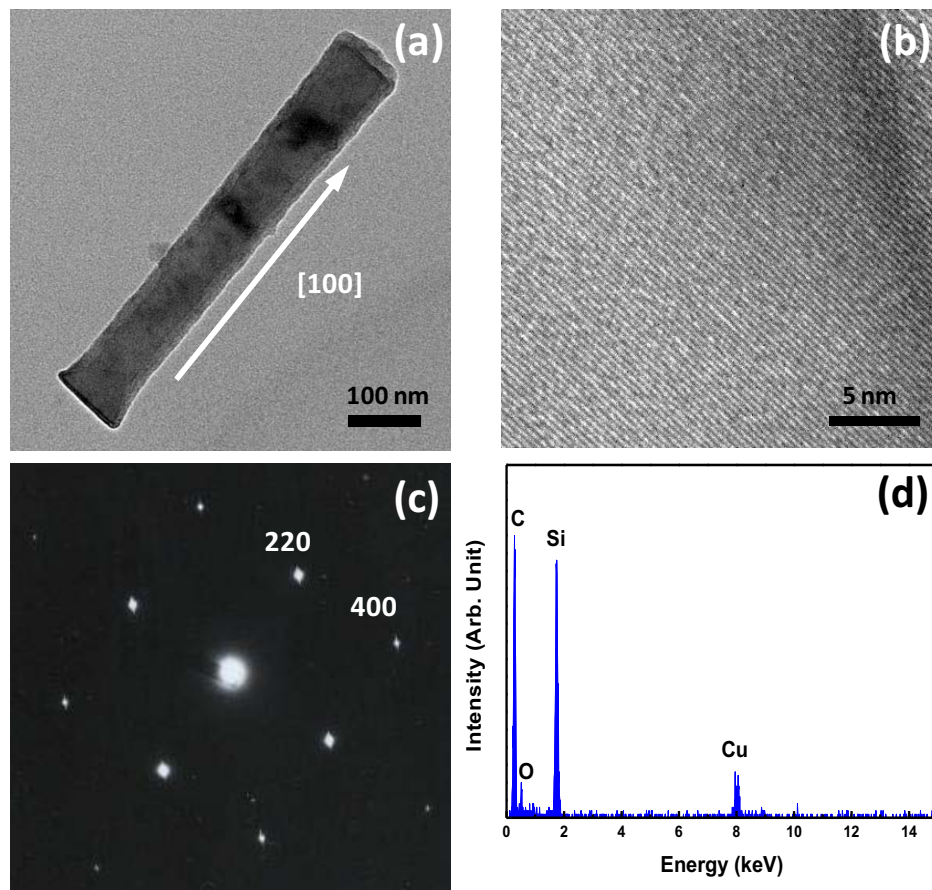


Figure 3. Low-magnification TEM image, (b) High resolution TEM image, (c) SAED pattern, and (d) EDS spectrum of the silicon nanowires.

Figure 4 displays the optical reflectances of the 0.5  $\mu\text{m}$ , 1  $\mu\text{m}$  silicon nanowires arrays and silicon substrate measured in a wavelength range of 200 ~ 1000 nm. The result reveals the 1- $\mu\text{m}$ -long SiNWs arrays have the lowest reflectance as compared with the others. It suggests that more photons were absorbed by the longer nanowire structure, which can be attributed to its high specific surface area and excellent light-trapping ability.

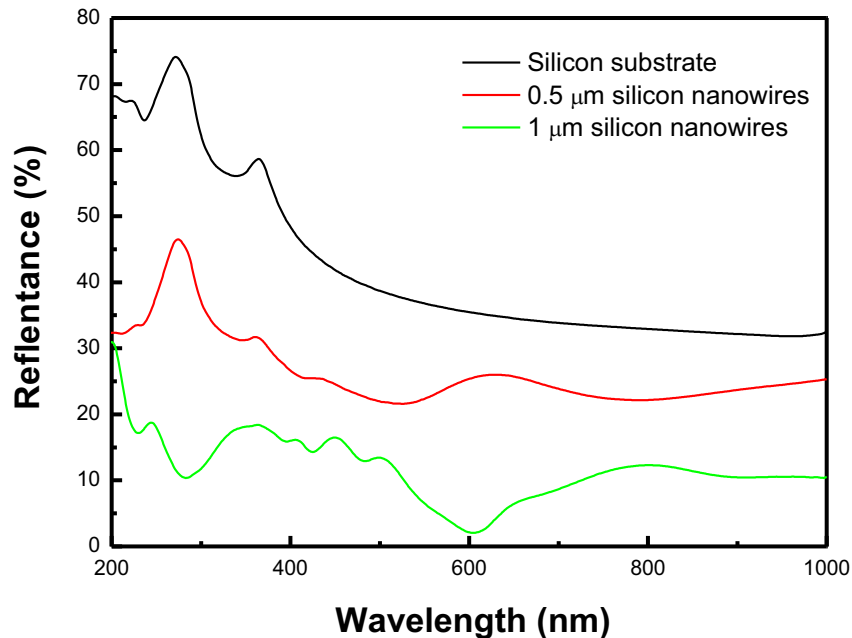


Figure 4. Optical reflectances of the 0.5  $\mu$  m, 1  $\mu$  m silicon nanowires and silicon substrate.

I-V characteristics of the SiNWs solar cell and the flat film solar cell under AM 1.5 simulated sunlight illumination are shown in Figure 5. With the intrinsic amorphous silicon thickness of 15 nm and n-layer thickness of 25 nm, the dependence of the PV properties on wire length has been discussed. The short-current density increased from 20.75 to 27.90 mA/cm<sup>2</sup>, the open circuit voltage ( $V_{OC}$ ) increased from 0.50 to 0.52 V, the fill factor (FF) decreased from 34.58 % to 32.39 % and the conversion efficiency increased from 3.59 to 4.69 % when the silicon nanowires length was increased from 0.5 to 1  $\mu$ m. Table I summarizes the PV properties of the coaxial-structured solar cells with SiNWs and the flat film solar cell. The enhancements in photocurrent and conversion efficiency were attributed to the nanowire structure. Furthermore, the PV performances exhibited that 1- $\mu$ m-long SiNWs arrays more effectively absorbed sunlight and increased the light trapping probability. On the other hand, the series resistance became larger and sheet resistance became smaller because of the longer wires. The result caused the decrements in the fill factor.

I-V characteristic of the flat film solar cell is also shown in Figure 5. The short-current density and the conversion efficiency of the flat film structure were 17.58 mA/cm<sup>2</sup> and 3.16 %, respectively. The proposed coaxial-structured solar cells with SiNWs exhibited nearly 58.70 % short-current density and 48.42 % efficiency enhancements over the flat film solar cell. The coaxial-structured solar cell has a shorter carrier transport path and radial transport direction which ensure that carriers reach the contact metal without significant recombination. Moreover, the nanowire structure has an anti-reflection property and enhances light absorption.

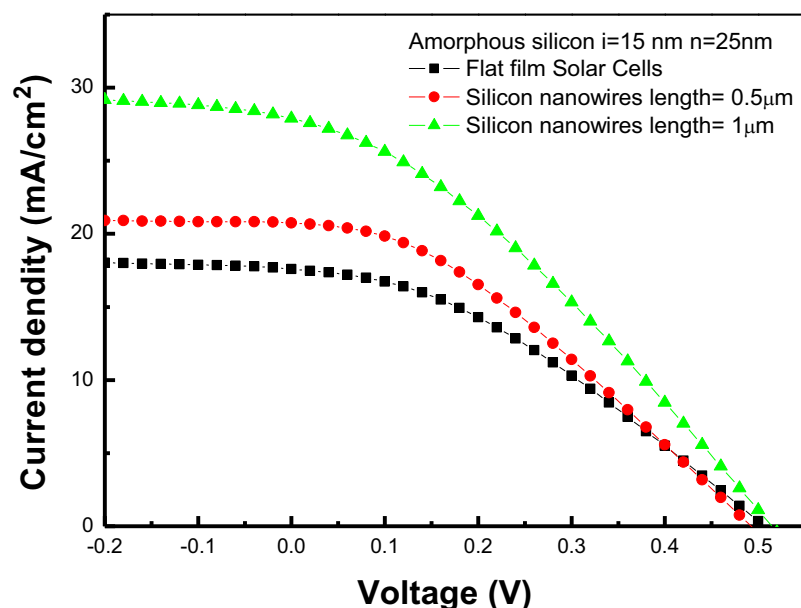


Figure 5. I-V characteristics of the silicon nanowires solar cell and the flat film solar cell.

**TABLE I.** Photovoltaic performances of the coaxial-structured solar cells with SiNWs and the plat film solar cell, short circuit current density ( $J_{sc}$ ), open circuit voltage ( $V_{oc}$ ), fill factor (FF), power conversion efficiency ( $\eta$ ).

	$J_{sc}$ (mA/cm <sup>2</sup> )	$V_{oc}$ (V)	FF (%)	$\eta$ (%)
Plat film	17.58	0.51	35.22	3.16
0.5 $\mu$ m SiNWs	20.75	0.50	34.58	3.59
1 $\mu$ m SiNWs	27.90	0.52	32.39	4.69

## Conclusions

Coaxial-structured solar cells with silicon nanowires were proposed by e-beam lithography and TCP-RIE method. The optical reflectances of the 0.5  $\mu$ m, 1  $\mu$ m silicon nanowires arrays and silicon substrate indicate that 1- $\mu$ m-long SiNWs arrays has the lowest reflectance. The short-current density increased from 20.75 to 27.90 mA/cm<sup>2</sup>, and the conversion efficiency increased from 3.59 to 4.69 % when the silicon nanowires length was increased from 0.5 to 1  $\mu$ m. The proposed coaxial-structured solar cells with SiNWs exhibited nearly 58.70 % short-current density and 48.42 % efficiency enhancements over the plat film solar cell, which is attributed to the enhanced light trapping probability and shortened carrier conduction path.

## Acknowledgments

This research was financially supported by the National Science Council of Taiwan under Contract No. NSC 99-2221-E-009-168-MY3. The authors would like to thank the Nano Facility Center (NFC) of National Chiao Tung University and the National Nano Device Laboratories (NDL) for technical supports.

## References

1. X.L. Chen, B.H. Xu, J.M. Xue, Y. Zhao, C.C. Wei, J. Sun, Y. Wang, X.D. Zhang, and X.H. Geng, *Thin Solid Films*, **515**, 3753(2007).
2. Y.R. Ryu, J.A. Lubguban, T.S. Lee, H.W. White, T.S. Jeong, C.J. Youn, and B.J. Kim, *Appl. Phys. Lett.* **90**, 131115(2007).
3. B. M. Kayes, H. A. Atwater, and N. S. Lewis, *J. Appl. Phys.* **97**, 114302 (2005).
4. Y. Zhang, L. W. Wang, and A. Mascarenhas, *Nano Lett.* **7**, 1264–1269 (2007).
5. L. E. M. Law, J. C. Johnson, Greene, R. Saykally and P. Yang, *Nat. Mater.* **4**, 455–459 (2005).
6. V. Sivakov, G. Andrä, A. Gawlik, A. Berger, J. Plentz, F. Falk, and S. H. Christiansen, *Nano Lett.*, Vol. **9**, No. 4 (2009)
7. Jin-Young Jung, Zhongyi Guo, Sang-Won Jee, Han-Don Um, Kwang-Tae Park, Moon Seop Hyun, Jun Mo Yang, and Jung-Ho Lee, *Nanotechnology*, 21, 445303 (2010).
8. S.E. Huq, L. Chen, and P.D. Prewett, *Microelectron. Eng.* **27**, 95 (1995).
9. Kuiqing Peng, Xin Wang, and Shuit-Tong Lee, *Appl. Phys. Lett.* **92**, 163103 (2008).
10. B. M. Kayes, M. A. Filler, M. C. Putnam, M. D. Kelzenberg, N. S. Lewis, and H. A. Atwater, *Appl. Phys. Lett.* **91**, 103110-103113 (2007).
11. Ling Xu, Wei Li, Jun Xu, Jiang Zhou, Liangcai Wu, Xian-Gao Zhang, Zhongyuan Ma, and Kunji Chen, *Applied Surface Science*, **255** 5414–5417 (2009).
12. Ching-Mei Hsu, Stephen T. Connor, Mary X. Tang, and Yi Cui, *Appl. Phys. Lett.* **93**, 133109 (2008).